Title

Identification of a GABAergic neuroblast lineage modulating sweet and bitter taste sensitivity.

Journal

Current Biology, 32(24)

Authors

Zhao, Yunpo

Duan, Jianli

Han, Zhe

et al.

Publication Date

2022-12-19

DOI

10.1016/j.cub.2022.10.029

Peer reviewed

HHS Public Access

Author manuscript

Curr Biol. Author manuscript; available in PMC 2023 December 19.

Published in final edited form as:

Curr Biol. 2022 December 19; 32(24): 5354–5363.e3. doi:10.1016/j.cub.2022.10.029.

Identification of a GABAergic neuroblast lineage modulating sweet and bitter taste sensitivity

Yunpo Zhao[1,2,3,5,*], **Jianli Duan**[1,3], **Zhe Han**[3], **Ylva Engström**[1], **Volker Hartenstein**[4,*]

[1]Department of Molecular Biosciences, The Wenner-Gren Institute, Stockholm University, 106 91 Stockholm, Sweden

[2]Biozentrum, University of Basel, 4056 Basel, Switzerland

[3]Center for Precision Disease Modeling, University of Maryland School of Medicine, Baltimore 21201, USA

[4]Department of Molecular, Cell and Developmental Biology, University of California, Los Angeles 90095-1606, USA

[5]Lead contact

SUMMARY

In *Drosophila melanogaster*, processing of gustatory information and controlling feeding behavior are executed by neural circuits located in the subesophageal zone (SEZ) of the brain.[1] Gustatory receptor neurons (GRNs) project their axons in the primary gustatory center (PGC), which is located in the SEZ.[1–4] To address the function of the PGC, we need detailed information about the different classes of gustatory interneurons that frame the PGC. In this work, we screened large collections of driver lines for SEZ inter-neuron-specific labeling and subsequently used candidate lines to access the SEZ neuroblast lineages. We converted 130 Gal4 lines to LexA drivers and carried out functional screening using calcium imaging. We found one neuroblast lineage, TRdm, whose neurons responded to both sweet and bitter tastants, and formed green fluorescent protein (GFP) reconstitution across synaptic partners (GRASP)-positive synapses with sweet sensory neurons. TRdm neurons express the inhibitory transmitter GABA, and silencing these neurons increases appetitive feeding behavior. These results demonstrate that TRdm generates a class of inhibitory local neurons that control taste sensitivity in *Drosophila*.

In brief

[*]Correspondence: ypzhao0407@gmail.com or yunpo.zhao@som.umaryland.edu (Y. Z.), volkerh@mcdb.ucla.edu (V. H.).

AUTHOR CONTRIBUTIONS

Conceptualization, Y.Z. and V.H.; methodology, Y.Z., V.H., and J.D.; investigation, Y.Z., J.D., and V.H.; writing—original draft, V.H. and Y.Z.; writing—review & editing, V.H., Y.Z., Y.E., and J.D.; funding acquisition, Y.E. and V.H.; resources, Y.E., Z.H., and V.H.; supervision, Y.E. and V.H.

DECLARATION OF INTERESTS

The authors declare no competing interests.

INCLUSION AND DIVERSITY

We support inclusive, diverse, and equitable conduct of research. Received: November 18, 2021

SUPPLEMENTAL INFORMATION

Supplemental information can be found online at https://doi.org/10.1016/j.cub.2022.10.029.

GABAergic neurons modulate chemosensation in *Drosophila*. Zhao et al. find that GABAergic neurons of neuroblast lineage TRdm in the central brain are activated by both sugar and bitter stimulation on the labellum. Silencing TRdm neurons increases appetitive feeding behavior while blunting aversive feeding behavior.

Graphical abstract

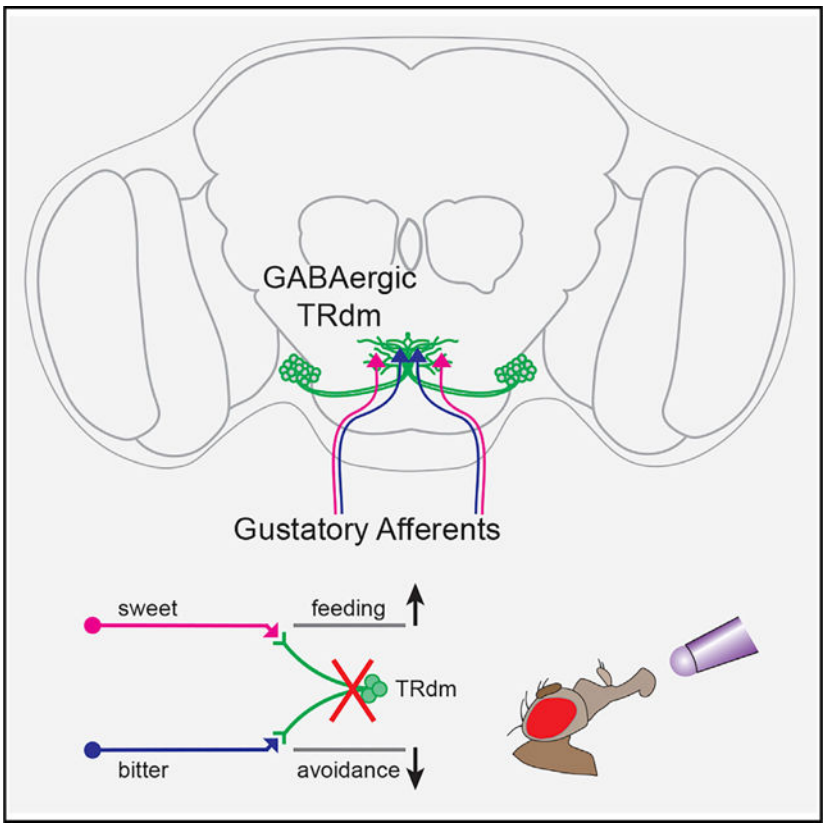

RESULTS

Neurons of the TRdm lineage are activated by sweet and bitter tastants

The sense of taste (gustation) plays a central role in guiding insect behavior, notably the initiation or inhibition of feeding, the search for and avoidance of food, grooming, mating, and oviposition.[1–5] Gustatory receptor neurons (GRNs) located in the mouth and pharynx, the proboscis, and the legs send their axons into the primary gustatory center (PGC) located in the subesophageal zone (SEZ) of the brain (Figures 1A and 1B). In flies, the immediate reflexive behaviors evoked by gustatory stimuli are the activation or inhibition of the extension of the proboscis and cibarial contraction, which pumps food into the stomach. Functional studies have defined the specific roles of motor neurons,[6,7] as well as those of numerous interneurons[8–13] that mediate behavioral effects in response to specific gustatory stimuli. Given that the SEZ is composed of several thousand neurons, it stands to reason that the already known interneurons involved in taste processing and feeding behavior represent but a small fraction of their overall number. In other sensory centers, notably the olfactory

center (antennal lobe), projection neurons (PNs) and local neurons (LNs) fall into relatively large classes that line up with defined neural lineages.[14–20] Whether a similar architecture, i.e., lineage-associated classes of projection and local interneurons, exists in the taste center has not yet been systematically addressed.

Our approach to identify SEZ lineages that generate clusters of gustatory interneurons that receive sensory input from the GRNs involved two steps (Figure 1C). In the first step, two Gal4 line collections, Janelia Flylight enhancer-Gal4 lines (AKA, GMR-Gal4 lines)[25] and Vienna Tiles (VT) enhancer-Gal4 lines,[26] which are built using genome-wide *cis*-regulatory modules (CRMs), provide genetic access to neuronal subpopulations. We prescreened the brain pattern of these drivers (about 13,000 lines) and chose 130 Gal4 lines that label sparse neurons in the SEZ or project neurites in the PGC for further study. Subsequently, we converted these Gal4 drivers to lineage-restricted LexA drivers,[27] taking advantage of the intersections of the CRM and the neuroblast (NB)-specific *dpn* promoter (denoted by CRM^dpn; Figures 1C and S1). Expression analysis of the converted lines in larval brains yielded 30 lines that label one to a few NB lineages. The CRM^dpn lines provide the potential for targeting specific NB lineages forming the SEZ. Since the lines will also aid in studies of other SEZ subpopulations, we present an atlas of the expression of 16 of these lines in Figures S2 and S3. Next, we had to convert the chosen CRM^dpn lines into line-age-restricted LexA drivers[27] expressed in mature nerve cells of the adult brain (Figures S1E and S1F), since the dpn promoter by itself is only expressed in the NB,[27] the stem cells of the developing fly brain.[28] To this end, we combined the CRM lines with a dpn^CRE cassette to activate LexA expression driven by a synaptobrevin (nSyb) promoter (Figure S1E; Awasaki et al.[27]) and used these lines to screen for the interneurons that receive taste input from the GRNs through calcium imaging (GCaMP6s,[29] a GFP-Calmodulin-M13 fusion protein). To elicit gustatory input, tastants were applied to the proboscis in living flies. In most of the tested lines (R14G08, R20D07, R23H04, R24E06, R51F01, R54H01, R81E08, VT206843, and VT207611), the basal level of the GCaMP signal was weak, or the projection pattern could not unambiguously be assigned to a specific lineage, likely because the depth of cell bodies and axon tracts in the brain tissue was too deep to be adequately resolved by the confocal microscope. By contrast, one driver line, VT206843^dpn>GCaMP6s, showed a significant taste-activated signal in a specific cluster of SEZ neurons located at the anterior apex of the SEZ, and thereafter we focused our study on this driver.

Anatomical analysis indicated that VT206843^dpn-positive neurons reacting to taste stimulation form part of lineage TRdm.[21] Cell bodies of TRdm form a dense cluster in the lateral cortex of the anterior SEZ; their fibers project medially as a tight bundle before entering the ventral tritocerebrum (TRv; called “prow” in studies conducted by Ito et al.[22] and Kendroud et al.[30]; Figures 1D–1G). Counts from 5 brains yielded an average of 55.6 (SD = 6.1) neurons per TRdm lineage per hemisphere. After entering the neuropil fibers of TRdm, neurons remain mostly restricted to the TRv where they overlap with the PGC (Figure 1G). VT206843^dpn>GFP brains showed expression in several other lineages of the SEZ and supraesophageal brain and VNC (Figure S4); none of these lineages, however, responded to taste stimulation. The construct is not expressed in any sensory afferents.

For TRdm, stimulation of the proboscis with 100 mM sucrose activated a GCaMP signal in both neuronal somata and neurites (Figures 2A and 2B) in satiated flies, indicating that the TRdm neurons form part of the *Drosophila* gustatory circuitry. Sucrose stimulation in starved flies also elicited strong neural activity (Figure 2C, top). The stimulation of the proboscis with a bitter compound, L-canavanine, activated a smaller subset of TRdm neurons. We counted the neurons that respond strongly and exclusively to sweet or bitter. The numbers are 2.5 ± 1.3 (n = 4) and 1.8 ± 1 (n = 4), respectively. Also, 5.8 ± 1.0 cells (n = 4) responded to both sweet and bitter. In the preparation shown in Figure 2C, cell 1 was activated by both sucrose and L-canavanine, whereas cell 2 was only activated by sucrose. We conclude that the TRdm neurons have functional connections with both sweet and bitter sensory neurons.

TRdm neurons are GABAergic neurons

Many LNs are traditionally considered to be inhibitory neurons, as shown for the olfactory system, where the vast majority of olfactory LNs are GABAergic.[31,32] Staining with antisera to γ-aminobutyric acid (GABA) showed fluorescence signal in all labeled TRdm neurons (Figures 3A and B–B″), revealing that the neurons in the lineage were GABAergic LNs. By contrast, staining for choline acetyltransferase (ChAT), which is considered to be an excellent marker for cholinergic neurons,[33] showed no signal in the TRdm neurons (Figure 3C).

TRdm neurons GRASP with sweet GRNs

Since the TRdm neurons are responsive to taste stimuli, we asked whether these neurons get direct synaptic input from taste receptor neurons. The multi-lineage expression pattern in the SEZ of VT206843^∧dpn makes this driver not ideal for a GFP reconstitution across synaptic partners (GRASP) experiment.[6,32] In search of more specific enhancer-Gal4 lines, we found one Gal4 line, R43G04, that labels a subset of TRdm neurons in the adult SEZ (Figure 3D). GCaMP6s peak fluorescence levels increased significantly in *R43G04* interneurons after stimulation with 100 mM sucrose (Figure 3E). Using R43G04-Gal4 and Gr5a-LexA drivers, we carried out GRASP-split GFP labeling. One half of split GFP (UAS-spGFP1–10) was expressed in R43G04 interneurons and the other half of GFP (LexAop-spGFP11) in sweet GRNs. To visualize neurites, *UAS-tdTomato* and *LexAop-HA* were expressed in these two neuronal populations, respectively (Figure 3F, inset). We detected spatial overlap and GRASP connections between R43G04 GABAergic neurons and sweet GRNs (Figures 3F and 3G) but not in the control brains (n = 5 and 3, respectively). 3D reconstructions of the spatial distribution of the GRASP signal relative to TRdm confirmed a restricted localization in regions of the PGC where the two neuronal populations were in close proximity (Figure 3H). These findings indicate that TRdm interneurons are directly contacted by sweet gustatory receptors.

No GRASP signal was observed when using Gr66a-LexA, expressed in bitter-sensing neurons[33] to drive LexAop-spGFP11. This could indicate that bitter-sensing neurons reach TRdm interneurons via an intermediary cell type (indicated by gray hatched arrow in Figure 4C); alternatively, there could be bitter-sensing afferents directly synapsing on a subset of TRdm interneurons that does not express R43G04.

VT206843^dpn modulates taste sensitivity

To further investigate whether the VT206843^dpn neurons are involved in taste perception, we performed proboscis extension response (PER) assays, expressing tetanus toxin (TNT) in these neurons (VT206843^dpn>LexAop-TNT) to silence their activity. Tastants were applied to the labellum or tarsi, which were referred to as labellar PER and tarsal PER, respectively (Figure 4A). In the labellar PER assays, the control satiated flies rarely extended their proboscis when tested with low concentrations of sucrose (1 or 10 mM), although they showed reliable proboscis extensions with 100 and 1,000 mM sucrose stimulation (Figure 4B). The expression of TNT in VT206843^dpn neurons significantly increased the PER in response to labellar stimulation with 1, 10, and 100 mM sucrose (Figure 4B), indicating that silencing VT206843^dpn neurons potentiated the PER in satiated flies. We next tested the feeding behavior in non-satiated flies. A 24-h starvation period increased the sweet appetite in control flies, as shown with the PER (Figure 4D). Silencing VT206843^dpn neurons further increased the sweet sensitivity (Figure 4D), implying the VT206843^dpn neurons control sweet sensitivity under satiated and starved conditions.

VT206843^dpn adjusts feeding behavior in response to diverse labellar taste stimuli

The findings outlined above indicate that TRdm may act as a circuit element involved in gain control for the sweet-sensing channel, dampening the PER-inducing output with increasing levels of sweet input (Figure 4C). On the other hand, as outlined above, some TRdm neurons also responded to bitter stimulation (Figure 2). Stimulation of bitter afferents is known to inhibit the PER.[34,35] We therefore asked whether this bitter sensitivity was also affected in VT206843^dpn>TNT flies. Since VT206843^dpn>TNT flies are much more sensitive to appetitive stimulation, compared with control flies, we needed a condition where we could induce a standardized PER before adding bitter compounds for the aversive PER test. The stimulation of the labellum with 100 mM sucrose induced 80%–90% of the PER in starved control flies, while 35 mM sucrose led to comparable PER in starved VT206843^dpn>TNT flies. Thus, we used these two conditions (100 mM sucrose + bitter for control flies; 35 mM sucrose + bitter for VT206843^dpn>TNT flies) for testing the bitter response in the labellar PER assays. Adding the bitter compound L-canavanine decreased the feeding behavior in an L-canavanine concentration-dependent manner in control flies. The inhibitory effect of L-canavanine was alleviated in VT206843^dpn>TNT flies (Figure 4E), demonstrating that VT206843^dpn neurons have the ability to strongly inhibit the PER triggered by sweet input. We further tested PER inhibition by denatonium, a compound that activates bitter receptor neurons but also directly inhibits sugar receptors.[36] We observed PER inhibition by denatonium in a similar pattern to that seen with L-canavanine (Figure 4F). However, with denatonium, the PER inhibition was affected much less in VT206843^dpn>TNT flies (Figure 4F), confirming similar previous results obtained by blocking $GABA_BR$.[35] We speculate that the strong inhibition of sweet receptors by denatonium predominates. Not only is the PER depressed, but input to the inhibitory TRdm neurons also decline. Consecutively, optogenetic silencing of TRdms has little or no additional effect.

Next, we performed tarsal PER to investigate VT206843^dpn neurons in taste perception. VT206843^dpn>TNT did not affect the feeding behavior with sucrose or L-canavanine

stimulation on the tarsus (Figures 4G–4I), indicating that VT206843^dpn neurons specifically modulate labellar taste perception but not tarsal taste sensitivity.

The effect of VT206843^dpn on taste sensitivity is attained by the TRdm lineage

Aside from TRdm, VT206843^dpn is also expressed in multiple other lineages (Figure S4). To demonstrate conclusively that the effect of VT206843^dpn neurons on feeding was mediated specifically by the TRdm neurons, we induced clones targeting individual lineages. We included Gal80 (tub>Gal80>) to block VT206843-Gal4 activity. The removal of Gal80 by flp recombinase in a stochastic manner[6] allowed us to recover subsets of VT206843^dpn-expressing lineages. The TRdm lineage was found in 16 of these flies, which showed significantly increased PER compared with the non-TRdm individuals (Figures 4J and 4K). By contrast, inhibiting other lineages (e.g., AL1, VLNP1, or the other SEZ lineages) did not show a correlation with feeding behavior. Thus, the clonal analysis confirmed that neurons of the TRdm lineage modulate labellar taste sensitivity in the *Drosophila* brain.

DISCUSSION

We here identified a cluster of local GABAergic neurons that corresponds to lineage TRdm and that modulates taste sensitivity. All TRdm neurons responded to sweet tastants, while a few neurons also showed activity upon bitter stimulants, demonstrating integration of sweet and bitter perception in these neurons. Prior to the current study, two publications have shed light on the role of inhibitory GABAergic neurons in the gustatory center of *Drosophila*. Pool et al.[37] identified a pair of descending GABAergic neurons, termed DSOG1 and DSOG2, that is required for regulating satiety. A follow-up study[38] confirmed that GABA plays a critical role in controlling satiety. The authors showed that one of the GABA-A receptors, resistant to dieldrin (RDL), is responsible for this effect; RNAi-mediated knockdown of RDL mimicked the phenotype resulting from DSOG1/DSOG2 inactivation.

Local inhibition has been studied in considerable detail for the insect olfactory system. Here, sensory afferents (olfactory receptor neurons [ORNs]) terminate in the antennal lobe, where they form ~50 glomeruli tuned to the specific odors. ORNs form synaptic connections with PNs as well as LNs that provide feedforward inhibition to PNs and feedback inhibition to ORNs.[39–41] Developmentally, LNs belong to two lineages, BAla2/ALv2 and BAlc/ALl1, each of which generates ~100 LNs per hemisphere.[42] Given their typically widespread innervation of multiple, if not all, glomeruli, LNs are broadly tuned to multiple odors. The role of lateral inhibition by LNs appears to be manifold. One important function is gain control: strong odor stimuli excite multiple glomeruli that will elicit a stronger inhibitory response, which in turns dampens the ORN and PN activity in any given glomerulus.[40,43–45] Lateral inhibition is also important to sharpen the tuning of a PN to a specific odor, thereby enhancing the diversity of odor responses in the PN population.[39,44] Finally, antennal lobe LNs mediating lateral inhibition are important for habituation.[17,46]

We propose that the GABAergic TRdm neurons, innervated by taste afferents in the PGC, perform a role similar to that of the inhibitory LNs of the antennal lobe. Thus, TRdm dendrites branch widely within the entire PGC, and our functional studies demonstrated

that in numerous cases, they react to both sweet and bitter stimuli (which are represented in different domains within the PGC). TRdm neurons inhibit feeding behavior (PER) in a concentration-dependent manner, with strong effects at low sucrose concentrations and weak or no effects at high concentrations (Figure 4), suggesting that their normal function may also form part of a gain control mechanism, as shown for the GABAergic olfactory LNs. The exact circuitry underlying this mechanism has not been worked out; thus, it is currently not known whether the inhibitory output of TRdm neurons (or other GABAergic neurons, such as those described in the study conducted by Chu et al. [35]) feeds back on gustatory afferents ("1" in Figure 4C) or forward on PNs ("2" in Figure 4C) or both, as in the antennal lobe.

Close parallels have been drawn between the circuitry of the olfactory system in insects and vertebrates, specifically regarding the role of local inhibitory loops.[47,48] The same argument can be made for the gustatory systems as well. Gustatory information reaches the hindbrain, where it is relayed via higher brainstem domains to the deep folds of the parietal cerebral cortex.[49–51] As in insects, taste information is integrated with a wide range of inputs from other external senses, as well as the visceral organs, and plays a central role in controlling feeding behavior. GABA-mediated inhibition, occurring at all stations of the gustatory pathway,[52–59] acts to sharpen the tuning of gustatory PNs. A wealth of pharmacological and behavioral studies (e.g., studies conducted by Stratford and Kelley[60] and Baldo et al.[61]) underscore the wide range of effects of GABA neurotransmission on food uptake-related behaviors.

Further studies of the *Drosophila* gustatory system will further our understanding of taste and taste-controlled behavior among all animal systems. The technologies developed over the past years allow for the recognition, followed by experimental manipulation, of the building blocks of a circuit such as the taste pathway, which in *Drosophila* mostly consist of small groups of neurons defined by their developmental-genetic history as lineages, hemilineages, or sublineages. Of great importance also is the availability of complete connectomes,[62,63] based on serial electron microscopy, of the *Drosophila* brain. The extraordinary importance of circuit reconstructions at single-synapse resolution for explaining functional data and prompting new hypotheses has been amply proven in studies investigating the *Drosophila* olfactory system, mushroom body, central complex, and motor system, to name but a few. We anticipate that connectomes currently in the making[62,63] will achieve similar insights into the circuitry underlying the processing of gustatory information in the SEZ.

STAR★METHODS

RESOURCE AVAILABILITY

Lead contact—Further information and requests for resources and reagents should be directed to and will be fulfilled by the Lead Contact, Yunpo Zhao (ypzhao0407@gmail.com; yunpo.zhao@som.umaryland.edu).

Materials availability—This study did not generate new unique reagents.

Data and code availability—Microscopy data reported in this paper will be shared by the lead contact upon request.

This paper does not report original code.

Any additional information required to reanalyze the data reported in this paper is available from the lead contact upon request.

EXPERIMENTAL MODEL AND SUBJECT DETAILS

***Drosophila* genetics—**Flies were raised on standard medium with 12-h light-dark cycles at 25 °C. The following fly lines were used: *VT206843-Gal4* (Vienna *Drosophila* Resource Center, VDRC), *Gr5a-LexA::VP16*, *Gr66a-LexA::VP16*, *LexAop-CD2::HRP*, *tub>Gal80>*, *UAS-CD4::spGFP1–10*, and *LexAop-CD4::spGFP11*,[6] *133LexAop2-IVS-GFP-p10* (Gerry Rubin), *hs-flp* (Bloomington Drosophila Stock Center, BDSC_58356), *UAS-CD4-tdTom* (BDSC_35841), *dpn(FRT.stop)LexA.p65* (BDSC_56162), *20xUAS-KD* (BDSC_55790), *R43G04-Gal4* (BDSC_49556), *dpn(KDRT.stop)cre.PEST* (BDSC_56164), *LexAop-rCD2-GFP* (BDSC_66544), *13XLexAop2-IVS-GCaMP6s-SV40* (BDSC_44589), and *nSyb(*loxP.stop*)LexA.p65* (BDSC_56166).

The following fly stocks were built for the screen: (1) *dpn(FRT.stop)LexA.p65; UAS-Flp/CyO; LexAop-CD2GFP/TM6B*, (2) *dpn(KDRT.stop)cre.PEST; 13 3LexAop2-IVS-GFP-p10/CyO; 20xUAS-KD, nSyb(loxP.stop)LexA.p65*, and (2) *dpn(KDRT.stop)cre.P-EST; 13 3LexAop2-GCaMP6s/CyO; 20xUAS-KD, nSyb(loxP.stop)LexA.p65*.

METHOD DETAILS

Immunohistochemistry—*Drosophila* brains were dissected in 1xPBS and fixed in 4% paraformaldehyde (pH7.4) for 30 min at room temperature, followed with washing in 1xPBST (0.3% Triton-X 100 in PBS) three times 15 min each. The specimens were blocked in 1% normal goat serum in PBST for 1 hour at room temperature, then incubated in primary antibody in blocking buffer at 4 °C for overnight. After 3×15 min washing in PBST, the specimens were stained with secondary antibody in blocking buffer for two hours at room temperature, then washed for 4×15 min in PBST and once in PBS before mounting. The following antibodies were used: mouse anti-Brp 1:20 (RRID: AB_2314866, DSHB), mouse anti-ChAT 1:1000 (4B1, RRID: AB_528122, DSHB), rabbit anti-GABA 1:2000 (A2052, Sigma-Aldrich), mouse anti-HRP 1:2000 (ab10183, RRID: AB_296913, Abcam), goat anti-rabbit Alexa Fluor 546, 1:400 (A-11035, Invitrogen), goat anti-mouse Alexa Fluor 546, 1:400 (A-11003, Invitrogen), and goat anti-mouse Alexa Fluor 647, 1:400 (A32733, Invitrogen).

3D Reconstruction—3D reconstruction of the SEZ of adult brain was performed using Fiji TrakEM2 plugin (https://imagej.net/plugins/trakem2/) according to the tutorials.

Behavior assays—For Proboscis Extension Response (PER) assay, newly eclosed female adults were aged for 3 days at 25 °C. A small piece of Kim-wipe tissue soaked with water was put in an empty vial. Flies were transferred to the vial (20–30 flies/vial) and starved for 22–24 hours at 25 °C. Satiated or starved flies were mounted for PER assay. For labellar

PER, flies were anesthetized on ice and mounted inside pipette tips that were cut in size so that only the head was exposed.[64] The mounted flies were positioned on a glass slide with double-sided tape, and allowed to recover in a humidified chamber for 1–2 hours. Before the test, flies were stimulated with water and allowed to drink until satiated. Flies were then stimulated on the labellum with tastants, using a 20-μL pipette tip attached to a 1-mL syringe.

For tarsal PER, flies were mounted on strips of myristic acid, they were allowed to recover in a humidified chamber for 1–2 hr. Before the test, flies were stimulated with water on the tarsi of the forelegs and allowed to drink ad libitum.

Clonal analysis—Virgin females of (dpn>KDRT-stop-KDRT>Cre:PEST; LexAop-GFP/CyO; 20xUAS-KDR.PEST, nSyb(loxP.stop)LexA.p65/TM6B) were crossed with (tub>Gal80>; tub>Gal80>/CyO; VT206843-Gal4, LexAop-TNT/TM6B) males. Embryos were collected in a 4-hour time window. A 30-min heat shock was carried out in a 37 °C water bath to induce chromosome recombination. Female adults of appropriate genotype were aged for 3 three days before behavior test. For the PER, each fly was tested 15 times with 35 mM sucrose + 100 mM L-canavanine on the labellum. Subsequent to each experiment, the expression pattern was analyzed individually. A total number of 77 flies were examined.

GCaMP imaging—GCaMP imaging was performed as previously described.[37] 3–7 days old female were anesthetized, and all legs were removed. The flies were mounted by insertion of the cervix into individual collars of a custom chamber. Nail polish was applied in a thin layer to seal the head. Melted wax was applied to adhere the fully extended proboscis to the chamber rim. The cuticle covering the SEZ was removed, and adult hemolymph like buffer was added into the preparation to cover the exposed brain. A cover slip was inserted to separate the proboscis from the preparation. GCaMP fluorescence was imaged with a Leica SP5 II confocal microscope equipped with a tandem scanner and HyD detector. The 25x water objective was used to visualize the SEZ. For each taste stimulation, images were acquired for 4 s prior to stimulation, approximately 1 s during stimulation, and 5 s after stimulation. Multiple focal planes were scanned with 1 frame per second instead of multi frames per second, because we wanted to include signal obtained from cell bodies, cell body fibers and terminal arborizations in our recordings.

QUANTIFICATION AND STATISTICAL ANALYSIS

Statistical analysis was performed with *t*-test with Welch's correction or two-way ANOVA with Tuckey correction, using GraphPad Prism 8.0 software. For the PER assays, 3 groups of data sets were generated (10–11 flies/group) for each genotype. Asterisks denote the statistical significance, **, $p<0.01$; ****, $p<0.0001$.

Supplementary Material

Refer to Web version on PubMed Central for supplementary material.

ACKNOWLEDGMENTS

We are grateful to Profs. Kristin Scott, Gerry Rubin, Chi-Hon Lee, and Mani Ramaswami; to the Bloomington Drosophila Stock Center (BDSC) and Vienna *Drosophila* Resource Center (VDRC) for providing fly strains; and to Susanne Flister (Basel University) for technical assistance. We want to particularly acknowledge the support and expert help of Heinrich Reichert, in whose laboratory Y.Z. conducted much of the research and who tragically passed away in 2019. This work was supported by the Swiss National Science Foundation and the Sinergia Program (CRSII3 136307) to V.H. and the Swedish Cancer Society (CAN 2017/524) and the Swedish Research Council (2018-04401) to Y.E.

REFERENCES

1. Dethier VG (1976). The hungry fly: a physiological study of the behavior associated with feeding. PLOS ONE 12. e0172886.
2. Melcher C, Bader R, and Pankratz MJ (2007). Amino acids, taste circuits, and feeding behavior in Drosophila: towards understanding the psychology of feeding in flies and man. J. Endocrinol. 192, 467–472. 10.1677/joe-06-0066. [PubMed: 17332516]
3. Masek P, and Keene AC (2016). Gustatory processing and taste memory in Drosophila. J. Neurogenet. 30, 112–121. 10.1080/01677063.2016.1185104. [PubMed: 27328844]
4. Scott K. (2018). Gustatory processing in Drosophila melanogaster. Annu. Rev. Entomol. 63, 15–30. 10.1146/annurev-ento-020117-043331. [PubMed: 29324046]
5. Chen YD, and Dahanukar A. (2020). Recent advances in the genetic basis of taste detection in Drosophila. Cell. Mol. Life Sci. 77, 1087–1101. 10.1007/s00018-019-03320-0. [PubMed: 31598735]
6. Gordon MD, and Scott K. (2009). Motor control in a Drosophila taste circuit. Neuron 61, 373–384. 10.1016/j.neuron.2008.12.033. [PubMed: 19217375]
7. Schwarz O, Bohra AA, Liu X, Reichert H, Vijayraghavan K, and Pielage J. (2017). Motor control of Drosophila feeding behavior. eLife 6, e19892. 10.7554/eLife.19892.
8. Yapici N, Cohn R, Schusterreiter C, Ruta V, and Vosshall LB (2016). A taste circuit that regulates ingestion by integrating food and hunger signals. Cell 165, 715–729. 10.1016/j.cell.2016.02.061. [PubMed: 27040496]
9. Marella S, Mann K, and Scott K. (2012). Dopaminergic modulation of sucrose acceptance behavior in Drosophila. Neuron 73, 941–950. 10.1016/j.neuron.2011.12.032. [PubMed: 22405204]
10. Kain P, and Dahanukar A. (2015). Secondary taste neurons that convey sweet taste and starvation in the Drosophila brain. Neuron 85, 819–832. 10.1016/j.neuron.2015.01.005. [PubMed: 25661186]
11. Jourjine N, Mullaney BC, Mann K, and Scott K. (2016). Coupled sensing of hunger and thirst signals balances sugar and water consumption. Cell 166, 855–866. 10.1016/j.cell.2016.06.046. [PubMed: 27477513]
12. Kim H, Kirkhart C, and Scott K. (2017). Long-range projection neurons in the taste circuit of Drosophila. eLife 6, e23386. 10.7554/eLife.23386.
13. Bohra AA, Kallman BR, Reichert H, and Vijayraghavan K. (2018). Identification of a single pair of interneurons for bitter taste processing in the Drosophila brain. Curr. Biol. 28, 847–858.e3. 10.1016/j.cub.2018.01.084. [PubMed: 29502953]
14. Jefferis GSXE, Marin EC, Stocker RF, and Luo L. (2001). Target neuron prespecification in the olfactory map of Drosophila. Nature 414, 204–208. 10.1038/35102574. [PubMed: 11719930]
15. Lai S-L, Awasaki T, Ito K, and Lee T. (2008). Clonal analysis of Drosophila antennal lobe neurons: diverse neuronal architectures in the lateral neuroblast lineage. Development 135, 2883–2893. 10.1242/dev.024380. [PubMed: 18653555]
16. Das A, Sen S, Lichtneckert R, Okada R, Ito K, Rodrigues V, and Reichert H. (2008). Drosophila olfactory local interneurons and projection neurons derive from a common neuroblast lineage specified by the empty spiracles gene. Neural Dev. 3, 33. 10.1186/1749-8104-3-33. [PubMed: 19055770]
17. Das A, Chiang A, Davla S, Priya R, Reichert H, Vijayraghavan K, and Rodrigues V. (2011). Identification and analysis of a glutamatergic local interneuron lineage in the adult Drosophila olfactory system. Neural Syst. Circuits 1, 4. 10.1186/2042-1001-1-4. [PubMed: 22330097]

18. Das A, Gupta T, Davla S, Prieto-Godino LL, Diegelmann S, Reddy OV, Raghavan KV, Reichert H, Lovick J, and Hartenstein V. (2013). Neuroblast lineage-specific origin of the neurons of the Drosophila larval olfactory system. Dev. Biol. 373, 322–337. 10.1016/j.ydbio.2012.11.003. [PubMed: 23149077]
19. Ito M, Masuda N, Shinomiya K, Endo K, and Ito K. (2013). Systematic analysis of neural projections reveals clonal composition of the Drosophila brain. Curr. Biol. 23, 644–655. 10.1016/j.cub.2013.03.015. [PubMed: 23541729]
20. Yu HH, Awasaki T, Schroeder MD, Long F, Yang JS, He Y, Ding P, Kao JC, Wu GY, Peng H, et al. (2013). Clonal development and organization of the adult Drosophila central brain. Curr. Biol. 23, 633–643. 10.1016/j.cub.2013.02.057. [PubMed: 23541733]
21. Hartenstein V, Omoto JJ, Ngo KT, Wong D, Kuert PA, Reichert H, Lovick JK, and Younossi-Hartenstein A. (2018). Structure and development of the subesophageal zone of the Drosophila brain. I. Segmental architecture, compartmentalization, and lineage anatomy. J. Comp. Neurol. 526, 6–32. 10.1002/cne.24287. [PubMed: 28730682]
22. Ito K, Shinomiya K, Ito M, Armstrong JD, Boyan G, Hartenstein V, Harzsch S, Heisenberg M, Homberg U, Jenett A, et al. (2014). A systematic nomenclature for the insect brain. Neuron 81, 755–765. 10.1016/j.neuron.2013.12.017. [PubMed: 24559671]
23. Miyazaki T, and Ito K. (2010). Neural architecture of the primary gustatory center of Drosophila melanogaster visualized with GAL4 and LexA enhancer-trap systems. J. Comp. Neurol. 518, 4147–4181. 10.1002/cne.22433. [PubMed: 20878781]
24. Pereanu W, and Hartenstein V. (2006). Neural lineages of the Drosophila brain: a three-dimensional digital atlas of the pattern of lineage location and projection at the late larval stage. J. Neurosci. 26, 5534–5553. 10.1523/JNEUROSCI.4708-05.2006. [PubMed: 16707805]
25. Jenett A, Rubin GM, Ngo TB, Shepherd D, Murphy C, Dionne H, Pfeiffer BD, Cavallaro A, Hall D, Jeter J, et al. (2012). A GAL4-driver line resource for Drosophila neurobiology. Cell Rep. 2, 991–1001. 10.1016/j.celrep.2012.09.011. [PubMed: 23063364]
26. Kvon EZ, Kazmar T, Stampfel G, Yáñez-Cuna JO, Pagani M, Schernhuber K, Dickson BJ, and Stark A. (2014). Genome-scale functional characterization of Drosophila developmental enhancers in vivo. Nature 512, 91–95. 10.1038/nature13395. [PubMed: 24896182]
27. Awasaki T, Kao CF, Lee YJ, Yang CP, Huang Y, Pfeiffer BD, Luan H, Jing X, Huang YF, He Y, et al. (2014). Making Drosophila line-age-restricted drivers via patterned recombination in neuroblasts. Nat. Neurosci. 17, 631–637. 10.1038/nn.3654. [PubMed: 24561995]
28. Homem CC, and Knoblich JA (2012). Drosophila neuroblasts: a model for stem cell biology. Development 139, 4297–4310. 10.1242/dev.080515. [PubMed: 23132240]
29. Chen TW, Wardill TJ, Sun Y, Pulver SR, Renninger SL, Baohan A, Schreiter ER, Kerr RA, Orger MB, Jayaraman V, et al. (2013). Ultrasensitive fluorescent proteins for imaging neuronal activity. Nature 499, 295–300. 10.1038/nature12354. [PubMed: 23868258]
30. Kendroud S, Bohra AA, Kuert PA, Nguyen B, Guillermin O, Sprecher SG, Reichert H, Vijayraghavan K, and Hartenstein V. (2018). Structure and development of the subesophageal zone of the Drosophila brain. II. Sensory compartments. J. Comp. Neurol. 526, 33–58. 10.1002/cne.24316. [PubMed: 28875566]
31. Chou YH, Spletter ML, Yaksi E, Leong JC, Wilson RI, and Luo L. (2010). Diversity and wiring variability of olfactory local interneurons in the Drosophila antennal lobe. Nat. Neurosci. 13, 439–449. 10.1038/nn.2489. [PubMed: 20139975]
32. Feinberg EH, Vanhoven MK, Bendesky A, Wang G, Fetter RD, Shen K, and Bargmann CI (2008). GFP Reconstitution Across Synaptic Partners (GRASP) defines cell contacts and synapses in living nervous systems. Neuron 57, 353–363. 10.1016/j.neuron.2007.11.030. [PubMed: 18255029]
33. Thistle R, Cameron P, Ghorayshi A, Dennison L, and Scott K. (2012). Contact chemoreceptors mediate male-male repulsion and male-female attraction during Drosophila courtship. Cell 149, 1140–1151. 10.1016/j.cell.2012.03.045. [PubMed: 22632976]
34. Wang Z, Singhvi A, Kong P, and Scott K. (2004). Taste representations in the Drosophila brain. Cell 117, 981–991. 10.1016/j.cell.2004.06.011. [PubMed: 15210117]

35. Chu B, Chui V, Mann K, and Gordon MD (2014). Presynaptic gain control drives sweet and bitter taste integration in Drosophila. Curr. Biol. 24, 1978–1984. 10.1016/j.cub.2014.07.020. [PubMed: 25131672]
36. Jeong YT, Shim J, Oh SR, Yoon HI, Kim CH, Moon SJ, and Montell C. (2013). An odorant-binding protein required for suppression of sweet taste by bitter chemicals. Neuron 79, 725–737. 10.1016/j.neuron.2013.06.025. [PubMed: 23972598]
37. Pool A-H, Kvello P, Mann K, Cheung SK, Gordon MD, Wang L, and Scott K. (2014). Four GABAergic interneurons impose feeding restraint in Drosophila. Neuron 83, 164–177. 10.1016/j.neuron.2014.05.006. [PubMed: 24991960]
38. Cheung SK, and Scott K. (2017). GABAA receptor-expressing neurons promote consumption in Drosophila melanogaster. PLOS One 12. e0175177. 10.1371/journal.pone.0175177.
39. Wilson RI, and Laurent G. (2005). Role of GABAergic inhibition in shaping odor-evoked spatiotemporal patterns in the Drosophila antennal lobe. J. Neurosci. 25, 9069–9079. 10.1523/JNEUROSCI.2070-05.2005. [PubMed: 16207866]
40. Olsen SR, and Wilson RI (2008). Lateral presynaptic inhibition mediates gain control in an olfactory circuit. Nature 452, 956–960. 10.1038/nature06864. [PubMed: 18344978]
41. Yaksi E, and Wilson RI (2010). Electrical coupling between olfactory glomeruli. Neuron 67, 1034–1047. 10.1016/j.neuron.2010.08.041. [PubMed: 20869599]
42. Chou Y-H, Spletter ML, Yaksi E, Leong JCS, Wilson RI, and Luo L. (2010). Diversity and wiring variability of olfactory local interneurons in the Drosophila antennal lobe. Nat. Neurosci. 13, 439–449. 10.1038/nn.2489. [PubMed: 20139975]
43. Asahina K, Louis M, Piccinotti S, and Vosshall LB (2009). A circuit supporting concentration-invariant odor perception in Drosophila. J. Biol. 8, 9. 10.1186/jbiol108. [PubMed: 19171076]
44. Olsen SR, Bhandawat V, and Wilson RI (2010). Divisive normalization in olfactory population codes. Neuron 66, 287–299. 10.1016/j.neuron.2010.04.009. [PubMed: 20435004]
45. Suzuki Y, Schenk JE, Tan H, and Gaudry Q. (2020). A population of interneurons signals changes in the basal concentration of serotonin and mediates gain control in the Drosophila antennal lobe. Curr. Biol. 30, 1110–1118.e4. 10.1016/j.cub.2020.01.018. [PubMed: 32142699]
46. Sudhakaran IP, Holohan EE, Osman S, Rodrigues V, Vijayraghavan K, and Ramaswami M. (2012). Plasticity of recurrent inhibition in the Drosophila antennal lobe. J. Neurosci. 32, 7225–7231. 10.1523/jneurosci.1099-12.2012. [PubMed: 22623667]
47. Hong EJ, and Wilson RI (2013). Olfactory neuroscience: normalization is the norm. Curr. Biol. 23, R1091–R1093. 10.1016/j.cub.2013.10.056. [PubMed: 24355783]
48. Zhu P, Frank T, and Friedrich RW (2013). Equalization of odor representations by a network of electrically coupled inhibitory interneurons. Nat. Neurosci. 16, 1678–1686. 10.1038/nn.3528. [PubMed: 24077563]
49. Lundy RF Jr., and Norgren R. (2004). Activity in the hypothalamus, amygdala, and cortex generates bilateral and convergent modulation of pontine gustatory neurons. J. Neurophysiol. 91, 1143–1157. 10.1152/jn.00840.2003. [PubMed: 14627662]
50. Simon SA, de Araujo IE, Gutierrez R, and Nicolelis MAL (2006). The neural mechanisms of gustation: a distributed processing code. Nat. Rev. Neurosci. 7, 890–901. 10.1038/nrn2006. [PubMed: 17053812]
51. Cho YK, and Li C-S (2008). Gustatory neural circuitry in the hamster brain stem. J. Neurophysiol. 100, 1007–1019. 10.1152/jn.01364.2007. [PubMed: 18525019]
52. Davis BJ (1993). GABA-like immunoreactivity in the gustatory zone of the nucleus of the solitary tract in the hamster: light and electron microscopic studies. Brain Res. Bull. 30, 69–77. 10.1016/0361-9230(93)90040-i. [PubMed: 8420636]
53. Smith DV, Li C-S, and Davis BJ (1998). Excitatory and inhibitory modulation of taste responses in the hamster Brainstema. Ann. N. Y. Acad. Sci. 855, 450–456. 10.1111/j.1749-6632.1998.tb10605.x. [PubMed: 9929638]
54. Kobashi M, and Bradley RM (1998). Effects of GABA on neurons of the gustatory and visceral zones of the parabrachial nucleus in rats. Brain Res. 799, 323–328. 10.1016/s0006-8993(98)00480-6. [PubMed: 9675328]

55. Ogawa H, Hasegawa K, Otawa S, and Ikeda I. (1998). GABAergic inhibition and modifications of taste responses in the cortical taste area in rats. Neurosci. Res. 32, 85–95. 10.1016/s0168-0102(98)00071-6. [PubMed: 9831255]

56. Brown M, Renehan WE, and Schweitzer L. (2000). Changes in GABA-immunoreactivity during development of the rostral subdivision of the nucleus of the solitary tract. Neuroscience 100, 849–859. 10.1016/s0306-4522(00)00355-9. [PubMed: 11036219]

57. Grabauskas G, and Bradley RM (2001). Postnatal development of inhibitory synaptic transmission in the rostral nucleus of the solitary tract. J. Neurophysiol. 85, 2203–2212. 10.1152/jn.2001.85.5.2203. [PubMed: 11353035]

58. Sharp AA, and Finger TE (2002). GABAergic modulation of primary gustatory afferent synaptic efficacy. J. Neurobiol. 52, 133–143. 10.1002/neu.10073. [PubMed: 12124751]

59. King MS (2003). Distribution of immunoreactive GABA and glutamate receptors in the gustatory portion of the nucleus of the solitary tract in rat. Brain Res. Bull. 60, 241–254. 10.1016/s0361-9230(03)00034-0. [PubMed: 12754086]

60. Stratford TR, and Kelley AE (1997). GABA in the nucleus accumbens shell participates in the central regulation of feeding behavior. J. Neurosci. 17, 4434–4440. 10.1523/jneurosci.17-11-04434.1997. [PubMed: 9151760]

61. Baldo BA, Alsene KM, Negron A, and Kelley AE (2005). Hyperphagia induced by GABAA receptor-mediated inhibition of the nucleus accumbens shell: dependence on intact neural output from the central amygdaloid region. Behav. Neurosci. 119, 1195–1206. 10.1037/0735-7044.119.5.1195. [PubMed: 16300426]

62. Dorkenwald S, McKellar C, Macrina T, Kemnitz N, Lee K, Lu R, Wu J, Popovych S, Mitchell E, Nehoran B, et al. (2020). FlyWire: online community for whole-brain connectomics. bioRxiv. 10.1101/2020.08.30.274225.

63. Scheffer LK, Xu CS, Januszewski M, Lu Z, Takemura SY, Hayworth KJ, Huang GB, Shinomiya K, Maitlin-Shepard J, Berg S, et al. (2020). A connectome and analysis of the adult Drosophila central brain. eLife 9, e57443. 10.7554/eLife.57443.

64. Shiraiwa T, and Carlson JR (2007). Proboscis extension response (PER) assay in Drosophila. J. Vis. Exp. 2007, 193. 10.3791/193.

Highlights

- *Drosophila* TRdm neuroblast lineage neurons respond to sweet and bitter tastants
- Neurons in the TRdm lineage are GABAergic
- The TRdm lineage arborizes in the primary gustatory center
- The TRdm lineage modulates taste sensation

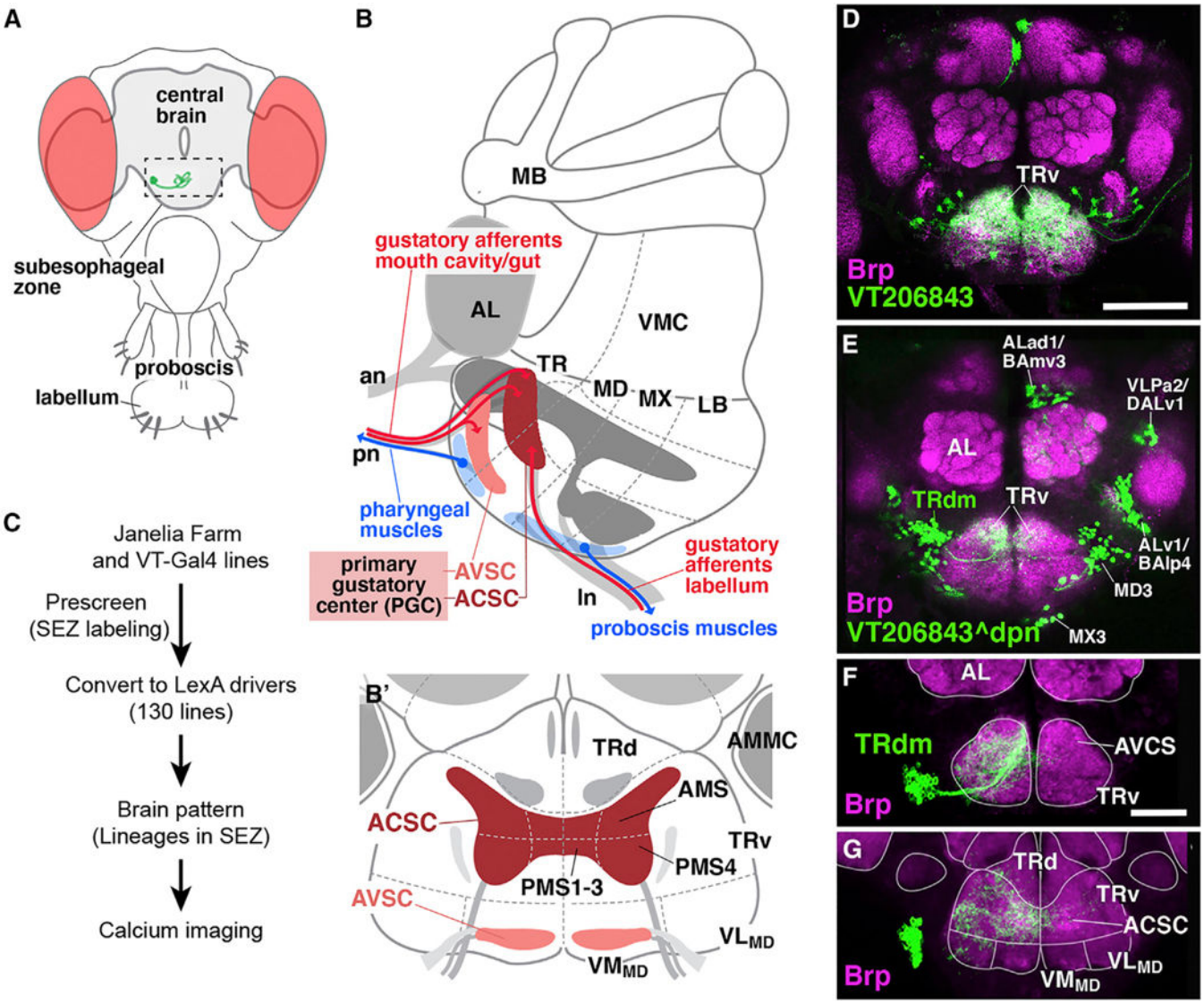

Figure 1. Interneurons of the *Drosophila* gustatory center

(A) Schematic representation of an adult *Drosophila* head with opening for calcium imaging indicated by hatched box.

(B and B′) Schematic lateral view (B) and anterior view (B′) of adult subesophageal zone (SEZ). Sensory nerves and compartments receiving gustatory input are rendered in red. Other sensory domains are shown in gray coloring. Blue shading outlines motor areas and motor axons to mouthparts. Hatched lines indicate segmental subdivision of SEZ.[21,22]

(C) Workflow. Janelia Farm and VT-Gal4 lines were screened. 130 Gal4 lines that label sparse neurons in the SEZ were converted to neuroblast- or neuroblast lineage-restricted LexA drivers. Calcium imaging was carried out to screen for the gustatory interneurons.

(D) Z projection of frontal confocal sections of *Drosophila* brain showing expression of VT206843 in clusters of neurons innervating the SEZ. Antibody to Bruchpilot (Brp) marks the neuropils (magenta).

(E) VT206843^dpn-driven expression of LexAop-GFP in multiple lineages, including TRdm, whose projection reaches the ventral domain of the tritocerebrum (TRv).
(F and G) GFP-labeled MARCM clone of TRdm lineage. Panels show z projections of frontal confocal sections near anterior tip of SEZ, which includes the anteroventral gustatory zone (AVSC) (F), and a plane 15 μm further posteriorly that houses the antero-central gustatory zone (ACSC) (G), which receives most taste afferents from the labellum and mouth cavity.
Abbreviations: ACSC, anterior central sensory center; AMS, anterior maxillary sensory domain as defined in the study conducted by Miyazaki and Ito[23]; AL, antennal lobe; AMMC, antenno-mechanosensory and motor center; an, antennal nerve; AVSC, anterior ventral sensory center; ALad1/BAmv3, ALlv1/BAlp4, VLPa2/DALv1, MD3, MX3, TRdm, neuroblast lineages (as defined in studies conducted by Ito et al.[19], Yu et al.[20], Hartenstein et al.[21], and Pereanu and Hartenstein[24]); LB, labium; ln, labial nerve; MB, mushroom body; MD, mandibula; MX, maxilla; PMS1–4, posterior maxillary sensory domains (as defined in the study conducted by Miyazaki and Ito[23]); pn, pharyngeal nerve; TR, tritocerebrum; TRd, dorsal tritocerebrum; TRv, ventral tritocerebrum; VL, ventrolateral neuropil domain; VM, ventromedial neuropil domain; VMC, ventromedial cerebrum.
Scale bars: 50μm in (D and E) and 25 μm in (F and G).
See also Figures S1–S3.

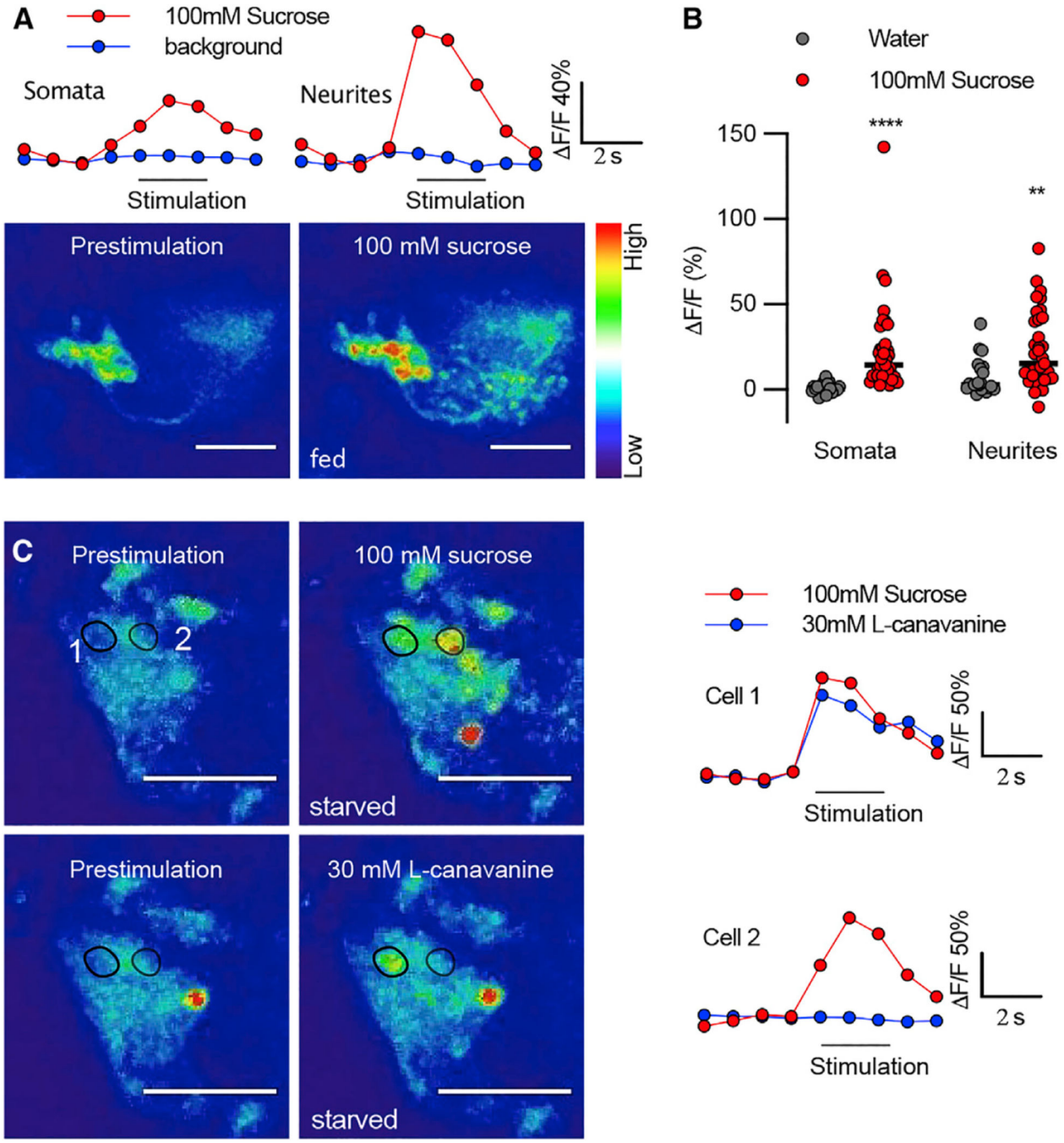

Figure 2. TRdm neurons are responsive to taste stimuli

(A) The TRdm cluster in the SEZ of VT2068 43^dpn>GCaMP6s brain responds to sucrose stimulation on the proboscis. Upper panels show the change of GCaMP6s fluorescence over time in the somata (left) and neurites (right). Lower panels present heatmaps of GCaMP6s fluorescence in VT20 6843^dpn>GCaMP6s SEZ.

(B) Average peak GCaMP6s fluorescence change in the interneurons following stimulation with sucrose and water, under fed condition.

(C) Calcium imaging of sweet- and bitter-evoked activity in the TRdm cell body cluster, along with traces showing the change in fluorescence over time in two ROIs, 1 and 2, in a starved fly. Based on size, ROIs likely correspond to single neuronal cell bodies; however, due to the limited resolution, they might occasionally also represent small groups of directly adjacent cell bodies. In the example shown, sucrose stimulation activated both 1 and 2, while L-canavanine evoked cell 1 only.

Scale bars: 25 μm. **$p < 0.01$; ****$p < 0.0001$.

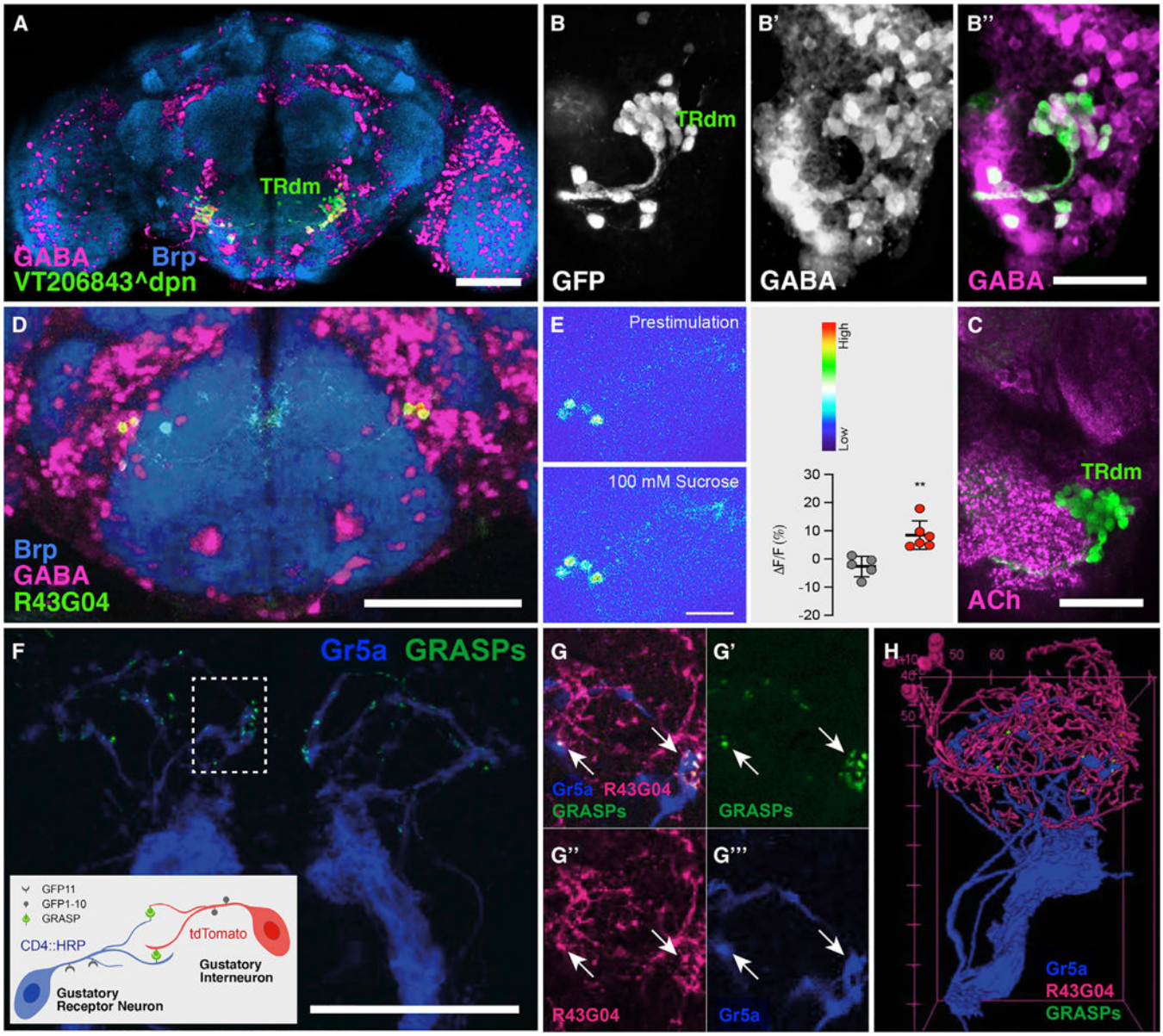

Figure 3. TRdm neurons are GABAergic and form GRASP connections with sweet GRNs

(A) Staining of a VT206843^dpn>GFP brain with anti-GABA (magenta). GABA is expressed in multiple brain lineages, including TRdm. Neuropil is labeled by anti-Brp (cyan).

(B–B″) Magnification of TRdm cluster expressing GABA.

(C) TRdm neurons do not overlap with ChAT-expressing cells.

(D) Staining of a R43G04-Gal4>GFP brain with anti-GABA (magenta), which labeled a subset of the TRdm neurons.

(E) Calcium imaging of 100 mM sucrose-evoked activity in the R43G04, along with traces showing the change in fluorescence over time.

(F and G) GRASP (green) shows contact between R43G04 GABAergic interneurons and Gr5a (sweet) axon terminals, shown in blue in boxed region (F) and in magnified view

in a single focal plane (G–G‴). Arrows point to GRASPs. Inset in (F) schematically illustrates GFP reconstitution between GRNs and interneurons. GRNs express splitGFP11 and CD4::HRP. Interneurons express splitGFP1–10 and tdTomato.

(H) Anterior view of a 3D reconstruction of one hemisphere of the brain shown in (F).

Scale bars: 50 μm in (A, C, and F) and 20 μm in (B and D). Error bars represent mean ± SD. **$p < 0.01$.

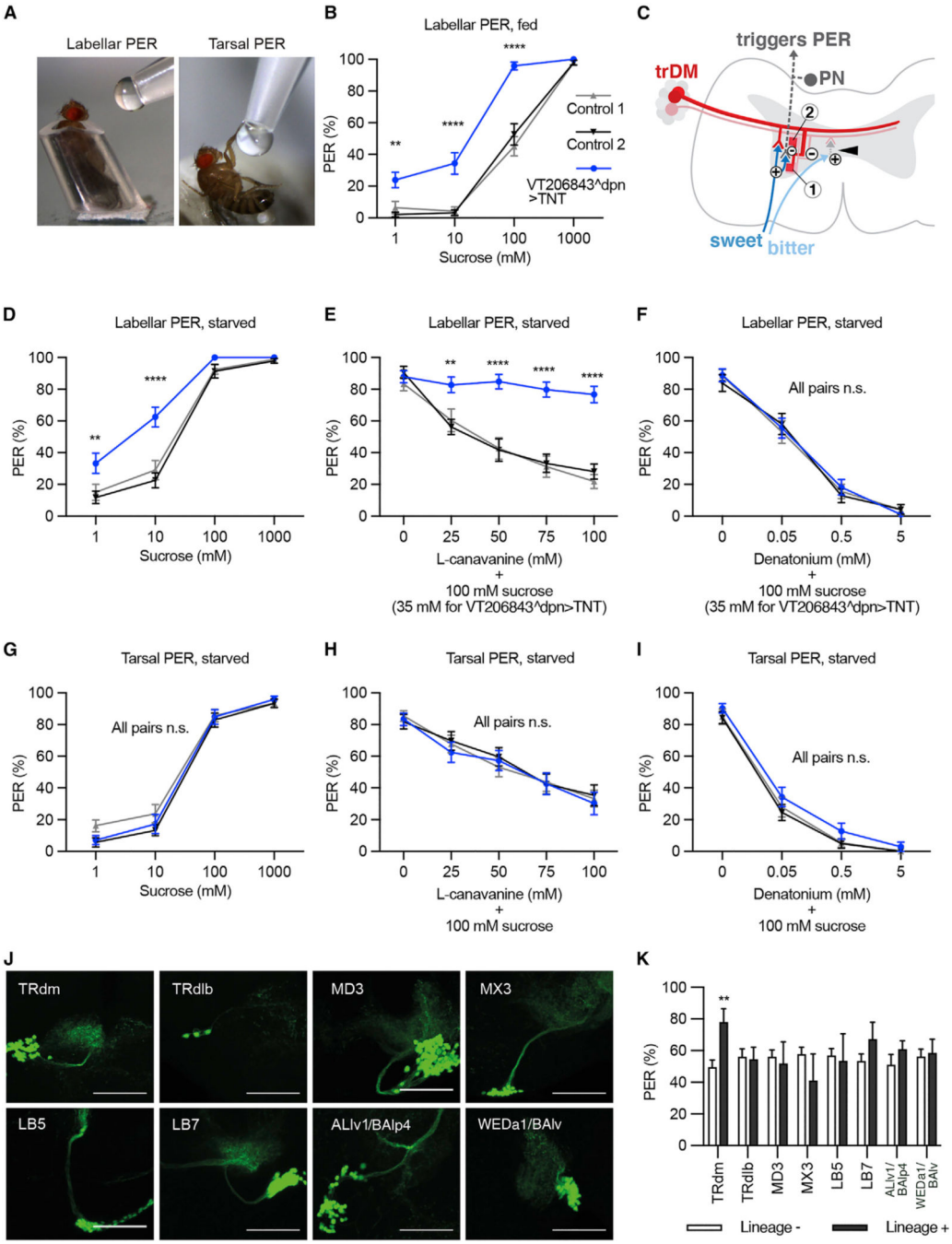

Figure 4. VT206843^dpn neurons modulate taste sensitivity

(A) Representative images of labellar PER (left) and tarsal PER (right) assays. In the labellar PER assay, tastants were applied to the proboscis. In the tarsal PER assay, tastants were applied to the tarsi of the first thoracic leg.

(B and D–F) Grouped plots showing the labellar PER of fed flies (B) and starved flies (D–F). Silencing VT206843^dpn neurons increased appetitive feeding response to sucrose stimulations (B and D), increased the PER to the sucrose plus L-canavanine (E) (hence decreased L-canavanine sensitivity), while it showed no effect to denatonium (F).

(C) Schematic representation of proposed interconnections between inhibitory TRdm neurons, sensory afferents, and output neurons modulating the PER. (G–I) Grouped plots showing the tarsal PER of starved flies. Silencing VT206843^dpn neurons did not affect the appetitive (G) or aversive (H and I) feeding behavior.

(J and K) Clonal analysis was performed to narrow down the lineage that mediates the feeding behavior. Shown are representative confocal images of the recovered lineages. All images are aligned with dorsal up. Scale bars: 50 μm. Each fly was stimulated with 35 mM sucrose + 100 mM L-canavanine for 15 times. The PER score was recorded and the brain pattern was analyzed individually. Fly genotypes: *dpn>KDRT-stop-KDRT>Cre:PEST/tub>Gal80>; LexAop-GFP/tub>Gal80>; 20xUAS-KDR.PEST, nSyb(loxP.stop)LexA.p65/VT206843-Gal4, LexAop-TNT*. In (K), graphs represent mean ± SEM and asterisks indicate significance by t test (**p < 0.01).

Abbreviations: ALlv1/BAlp4, LB5, LB7, MD3, MX3, TRdl, TRdm, WEDa1/Balv, neuroblast lineages (as defined in studies conducted by Ito et al.[19], Yu et al.[20], Hartenstein et al.[21], and Pereanu and Hartenstein[24]); PN, projection neuron.

Scale bars: 50 μm. Error bars represent mean ± SEM. **p < 0.01; ****p < 0.0001.

See also Figure S4.

KEY RESOURCES TABLE

REAGENT or RESOURCE	SOURCE	IDENTIFIER
Antibodies		
Mouse monoclonal anti-Brp	Developmental Study Hybridoma Bank	Cat# Nc82; RRID: AB_2314866
Mouse monoclonal anti-ChAT	Developmental Study Hybridoma Bank	Cat# 4B1; RRID: AB_528122
Mouse monoclonal anti-HRP	Abcam	Cat# ab10183; RRID: AB_296913
Rabbit anti-GABA	Sigma-Aldrich	Cat# A2052; RRID:AB_477652
Goat anti-rabbit Alexa Fluor 546	Invitrogen	Cat# A-11035; RRID:AB_143051
Goat anti-mouse Alexa Fluor 546	Invitrogen	Cat# A-11003; RRID:AB_141370
Goat anti-mouse Alexa Fluor 647	Invitrogen	Cat# A32733; RRID:AB_2633282
Experimental models: Organisms/strains		
Drosophila melanogaster. w^{1118}	Bloomington Drosophila Stock Center (BDSC)	RRID:BDSC_3605
Drosophila melanogaster. tub>Gal80>/CyO; TM2/TM6B	BDSC	RRID:BDSC_38880
Drosophila melanogaster. 13XLexAop2-IVS-GCaMP6s-SV40	BDSC	RRID:BDSC_44589
Drosophila melanogaster. 20xUAS-KD	BDSC	RRID:BDSC_55790
Drosophila melanogaster. UAS-CD4-tdTom	BDSC	RRID:BDSC_35841
Drosophila melanogaster. dpn(FRT.stop)LexA.p65	BDSC	RRID:BDSC_56162
Drosophila melanogaster. R43G04-Gal4	BDSC	RRID:BDSC_49556
Drosophila melanogaster. LexAop-CD2::HRP	BDSC	RRID:BDSC_56523
Drosophila melanogaster. dpn(KDRT.stop)cre.PEST	BDSC	RRID:BDSC_56164
Drosophila melanogaster. lexAop-rCD2-GFP	BDSC	RRID:BDSC_66544
Drosophila melanogaster. nSyb(loxP.stop)LexA.p65	BDSC	RRID:BDSC_56166
Drosophila melanogaster. 13×LexAop2-IVS-GFP-p10	Gerry Rubin	N/A
Drosophila melanogaster. Gr5a-LexA::VP16	Kristin Scott[6]	N/A
Drosophila melanogaster. Gr66a-LexA::VP16	Kristin Scott[6]	N/A
Drosophila melanogaster. UAS-CD4::spGFP1–10	Kristin Scott[6]	N/A
Drosophila melanogaster. LexAop-CD4::spGFP11	Kristin Scott[6]	N/A
Drosophila melanogaster. VT206843-Gal4	Vienna Drosophila Resource Center (VDRC)	206843
Software and algorithms		
Adobe Illustrator CS6 version	https://www.adobe.com/	CC2018
FIJI (ImageJ)	https://imagej.net/Fiji/Downloads	Fiji-macOS
GraphPad Prism	https://www.graphpad.com/scientific-software/prism/	8.2.1